Irreversible aggregation of interacting particles in one dimension

Hachem Sidi Ammi,[1] Anna Chame,[2,*] M'hammed Touzani,[1] Abdelilah Benyoussef,[1,†] Olivier Pierre-Louis,[3,‡] and Chaouqi Misbah[3,§]

[1]*Département de Physique, Faculté des Sciences, Université Mohammed V, Agdal, Avenue Ibn Batouta, Boîte Postale 1014 Rabat, Morocco*

[2]*Instituto de Física, Universidade Federal Fluminense, Avenida Litorânea s/n, 24210-340 Niterói RJ, Brazil*

[3]*Laboratoire de Spectrometrie Physique—THESHE, CNRS, UJF–Grenoble I, Boîte Postale 87, F-38402 Saint Martin d'Hères, France*

(Received 25 August 2004; published 1 April 2005)

We present a study of the aggregation of interacting particles in one dimension. This situation, for example, applies to atoms trapped along linear defects at the surface of a crystal. Simulations are performed with two lattice models. In the first model, the borders of atoms and islands interact in a vectorial manner via force monopoles. In the second model, each atom carries a dipole. These two models lead to qualitatively similar but quantitatively different behaviors. In both cases, the final average island size S_f does not depend on the interactions in the limits of very low and very high coverages. For intermediate coverages, S_f exhibits an asymmetric behavior as a function of the interaction strength: while it saturates for attractive interactions, it decreases for repulsive interactions. A class of mean-field models is designed, which allows one to retrieve the interaction dependence on the coverage dependence of the average island size with a good accuracy.

DOI: 10.1103/PhysRevE.71.041603 PACS number(s): 68.43.Jk, 81.10.Aj, 68.55.Ac

I. INTRODUCTION

Submonolayer growth—the deposition of less than one monolayer of atoms on a crystal surface—has attracted much interest [1–5] in the past decade. This interest was first triggered by the search for a better understanding of the initial stages of thin-film growth, which drastically influences the later stages of growth. Another research focus for submonolayer growth is the formation of novel nanostructures, such as quantum wires along crystal steps [6–9].

The submonolayer regime is dominated by the deposition and diffusion of adatoms and the formation and growth of islands, through nucleation, coalescence, and capture of new adatoms. Another possible relevant factor is the presence of long-range elastic interactions between adatoms. The interaction free energy between two adatoms deposited on a surface, separated by the distance r, is of the form $E(r) \sim 1/r^3$ [10] and is repulsive. This repulsive character is due to the local deformation that an adatom creates in the substrate, which gets smaller with the distance from the site in which this adatom is placed. If another adatom arrives, it tries to be where the deformation of the substrate is smaller, i.e., far away from the first adatom. As will be seen later, in reality the interaction law is more complex and attraction may arise as well. Beyond the submonolayer regime, elastic relaxation may be responsible for the formation of mounds in the growing film, since in this way a coherent (undislocated) three-dimensional island can relax its stress.

Apart from the elastic repulsion between adatoms which are in different sites, there are also direct chemical interactions between them, which are strong and in general attractive. There is competition between the long-range elastic repulsion and the short-range attraction. The elastic interaction is in general weaker for isolated atoms, but can become important for islands [1].

Recently, several models of island growth under the influence of long-range interactions (not necessarily of elastic origin) have been considered, using computational simulations and scaling arguments. For instance, Tataru *et al.* [11] considered attractive and repulsive interactions between adatoms of the form $1/r$ in a postdeposition (diffusion only after deposition) model of island growth in one- and two-dimensional substrates. Steinbrecher *et al.* [12] considered the growth of fractal clusters under a diffusion-limited aggregation (DLA) process with elastic interactions (of the form $1/r^3$). Similarly, Indiveri *et al.* [13] used attractive potentials of the form $1/r^\alpha$ to consider the influence of long-range interactions in the growth of a DLA aggregate. Very recently, a model of submonolayer island formation with repulsive elastic interactions of the form $1/r^3$ in a two-dimensional substrate was considered by Gutheim *et al.* [14]. In their model, diffusion occurs simultaneously with deposition, and monomers can be deposited on top of existing islands. The islands become stable when a dimer is formed (critical nucleation size $i=1$). In the regime of low coverages, they observed that, when the ratio between the elastic interaction and the temperature increases, the density of monomers continues to grow until greater values of the coverage is reached, and so island nucleation is deferred to higher coverage values when the elastic interaction increases. Another recent work [15], using the same repulsive elastic energy between adatoms, considered a variant of the model of submonolayer island growth (in a one-dimensional substrate) in which only the adatom that is being deposited at each time diffuses (until it reaches the local minimum of the energy) under the influence of the temperature and the repulsive interaction between particles, while the rest of the system is frozen. They only con-

*Electronic address: achame@if.uff.br

†Electronic address: benyous@fsr.ac.ma

‡Electronic address: olivier.pierre-louis@ujf-grenoble.fr

§Electronic address: chaouqi.misbah@ujf-grenoble.fr

sidered the case of stable dimers and coverages above 0.2. They found a maximum on the island size distribution that corresponds to greater island sizes as the coverage increases. In their model, the temperature does not have a great influence on the island size distribution.

It turns out that in all the above studies, elastic interaction was considered to be scalar, and this strongly differs from what occurs in real situations. It is not obvious that these studies should apply to heteroepitaxial growth. For example, in Ref. [15], it was considered that all the atoms within an island interact with adatoms with a law $1/r^3$. The same reasoning was applied in Ref. [14]. In reality, the elastic interaction is vectorial, and the effect of an island is localized along the periphery only: the periphery is a location of force monopoles [16,17]. Of course this result follows from integration of the elastic interaction $1/r^3$ over the island, and it is only when the interaction is treated vectorially that the contributions within the island cancel. In Ref. [11], only diffusing particles are supposed to interact, but no interaction, either between an adatom and the island periphery or between two islands, was taken into consideration. In view of this situation, it is desirable to clarify how elasticity must be taken into account. This is the first goal of this paper.

We shall then apply our results to one-dimensional (1D) aggregation by means of Monte Carlo simulations. By one dimensional we mean a line lying on a 2D substrate, like a quantum wire forming along, for example, a monatomic step. Some experimental observations of such structures are given in Refs. [6–9]. We shall see that generically the interaction between two 1D islands contains contributions like $1/r^3$ stemming from atom-atom interactions within the two islands, as well as $1/r$ interactions between the edges of the islands (if we extend our scheme to growth of 2D islands, then only contributions from the peripheries survive).

Diffusion and nucleation in the postdeposition regime were observed in several experiments [21,22]. This is taken to mean that the deposition process is performed at low enough temperatures [22] so that adatom diffusion is slow during deposition (deposition is made on a time scale for which organization into islands is not yet effective), then the flux is shut off, and adatom rearrangement into islands occurs. Significant mass transport and formation of islands after deposition can also be obtained by annealing the sample [7]. We shall consider irreversible aggregation here and adopt the case where a dimer is stable. The other situations, like simultaneous growth and nucleation, as well as strong annealing leading to desorption, or the allowance for a minimal size for the stability of nuclei, will constitute the subject of future work. We hope thus that our understanding of self-organization can be accomplished by a progressive refinement of the model.

This paper is organized as follows. In the next section, we present a brief revision about elastic interactions. In Sec. III, we describe the system under consideration and related experiments. In Sec. IV, we present the details of the model used, and the simulation technique. Some tools for the analysis, such as the scaling hypothesis and the island correlation function, are presented in Sec. V. Then the results of the simulations are presented in Sec. VI. We finally analyze the results using a mean-field model in Sec. VII, and discuss the limit of low coverage in Sec. VIII with the help of a point island model.

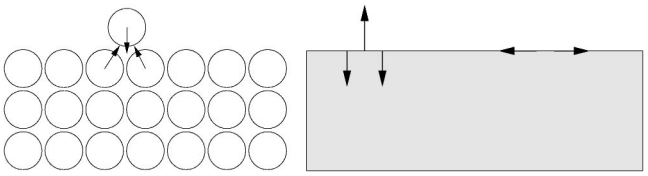

FIG. 1. An adatom on a surface and the forces on the substrate.

II. A BRIEF SURVEY ON ELASTIC INTERACTIONS

An adatom on a surface creates forces on the substrate, and due to the action-reaction principle, the substrate reacts by a set of forces that cancel the total force (Fig. 1). In addition, the total torque must be zero. The total interaction energy between two adatoms can be written in terms of a sum of interactions between individual forces. This has the form [16]

$$\mathcal{E}_{\mathrm{int}} = -\frac{1+\sigma}{\pi E}\left(\frac{1-\sigma}{r}\mathbf{f}_1\cdot\mathbf{f}_2 + \frac{\sigma}{r^3}(\mathbf{r}\cdot\mathbf{f}_1)(\mathbf{r}\cdot\mathbf{f}_2)\right), \qquad (1)$$

where σ is the Poisson ratio and E is the Young modulus. Note that in Ref. [16], the total minus sign is missing. In order to describe precisely how the interaction energy must be written, we assign to each atom (be it free or in an island) a set of forces and then use directly the above expression. For an island of atoms of B nature on top of a substrate of A nature, one can show analytically [16] that for an island the effect follows from a set of forces coming from the periphery only. This effect, as discussed in the Introduction, owes its origin to the vectorial character of the interaction (see Fig. 2).

Let us specialize the general expression (1) to simple situations. If two forces lie along the separation vector and have the same sign [Fig. 3(a)], then we easily find that

$$\mathcal{E}_{\mathrm{int}}^{\mathrm{force}} = -A_{\parallel}/r, \qquad (2)$$

where $A_{\parallel} \equiv (1+\sigma)f^2/(\pi E)$. The interaction is thus attractive. If the forces are antiparallel, then obviously the interaction would be repulsive [Fig. 3(b)].

Let us suppose now that there is a force doublet [Fig. 3(c)] pointing along $\mathbf{r}$. Then we obtain for the interaction energy

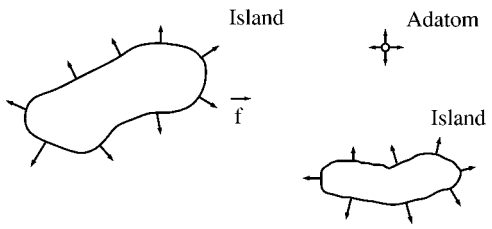

FIG. 2. Islands and adatoms on a substrate. For 2D islands, only interactions between the peripheries survive.

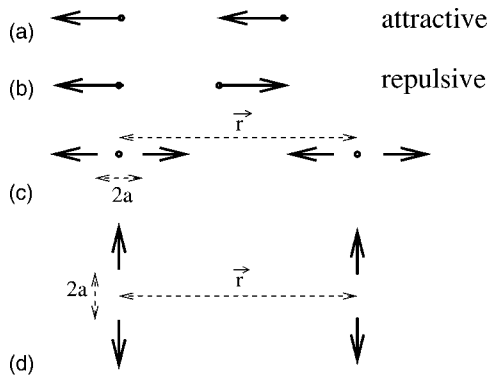

FIG. 3. (a) Parallel forces, (b) antiparallel forces, (c) force doublet along $\vec{r}$, and (d) force doublet orthogonal to $\vec{r}$.

$$\mathcal{E}_{\rm int}^{d} = \frac{8A_{\parallel}a^2}{r^3}, \tag{3}$$

which is a repulsive interaction [17]. This is the classical Kohn-Lau interaction [10]. If, however, the doublet is orthogonal to **r** [Fig. 3(d)], we obtain

$$\mathcal{E}_{\rm int}^{d} = -\frac{4A_{\parallel}(1-3\sigma)a^2}{r^3}. \tag{4}$$

If $\sigma<1/3$ (the usual range for σ lies within $0.25<\sigma<0.3$), the interaction is attractive; it is repulsive otherwise. These simple examples show clearly that the interaction energy must be treated accurately depending on the situation under consideration.

III. THE SYSTEM UNDER CONSIDERATION

We restrict ourselves to 1D patterns in the postdeposition case. That is, N atoms are randomly deposited along a chain and then, after the deposition flux has been shut off, diffusion takes place in the presence of elastic interactions. As a realistic 1D system, we have in mind a nucleation process occurring along a step on a high-symmetry surface, or on a vicinal surface. The latter situation is often used for the fabrication of quantum wires. Many experiments indeed report on the formation of chains of atoms [6], molecules [7], or clusters [8] along steps. Moreover, experiments [18] show that, in the case of atom chains [6], atoms diffuse along steps, and do not detach from the steps at room temperature. Sometimes, more complex structures appear along the steps, such as platelets [9], dots [7], or rough stripes [6]. Furthermore, the formation of one-dimensional self-organized nanostructures on patterned substrates [19,20] has recently been observed in experiments. To our knowledge, the dynamics of formation and annealing of the chains has not been modeled yet in the literature. Here we focus on a basic situation, with a single wire before the completion of a monorow: the 1D coverage denoted as θ hereafter is such that $\theta<1$.

According to the last section, the elastic effect due to heteroepitaxy of an island corresponds to a set of forces lying on the periphery of the wire, as schematically shown in Fig. 4(a). In that figure, we show both islands and adatoms. We

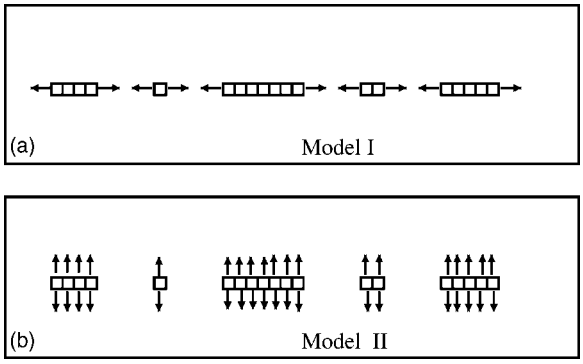

FIG. 4. (a) Model I, in which only horizontal forces are considered, and (b) model II, with perpendicular forces only.

suppose here that islands having two atoms are stable. Thus, in principle, one has to consider interactions between parallel and perpendicular forces, according to expression (1). In order to gain a better qualitative understanding, we shall separately analyze the situations with (i) only the horizontal forces and (ii) only the perpendicular ones. These two models will be referred to as models I and II, respectively. We shall also consider both attractive and repulsive interactions.

IV. MODELS

We consider a one-dimensional chain on which the occupation numbers σ_n are defined. $\sigma_n=0$ or $\sigma_n=1$ when the site n is, respectively, empty or filled with an atom.

Let us first consider model I. In order to account for the vectorial character of the forces exerted by the atoms on the substrate, we shall write that each atom at the site n leads to two opposite forces at $n+1/2$ and $n-1/2$. Thus, between two neighboring atoms at n and $n+1$, the sum of the forces exerted at $n+1/2$ is zero. The only nonvanishing forces will be at the borders of islands or isolated atoms. These forces will interact according to Eq. (2), and the total energy of the system reads

$$E = -\epsilon\sum_{n}\sigma_n\sigma_{n+1} - A_{\parallel}\sum_{n>m}(\sigma_n-\sigma_{n+1})(\sigma_m-\sigma_{m+1})\frac{1}{|n-m|}, \tag{5}$$

where ϵ is the bond energy and $A_{\parallel}$ is the prefactor of the elastic interaction.

We now turn to model II. In this case, all atoms interact with each other via dipole-dipole interactions, and the total energy reads

$$E = -\epsilon\sum_{n}\sigma_n\sigma_{n+1} + A_{\perp}\sum_{n>m}\frac{\sigma_n\sigma_m}{|n-m|^3}, \tag{6}$$

where $A_{\perp}=4A_{\parallel}(1-3\sigma)a^2$ from Eq. (4).

In both models, two distant clusters have an interaction energy $\sim 1/r^3$. Nevertheless, the details of the interactions are different. As we shall see in the following, these differences may lead to significant changes in the overall behavior.

These models were implemented in a simple way. Adatoms are deposited onto a one-dimensional substrate, with a

probability θ at each site, so that the coverage is θ. If none of the nearest-neighbor sites of an atom is occupied, the atom is called an adatom, and it is allowed to move. The attachment to an island is set to be irreversible: atoms with one or two nearest neighbors do not move. For this regime to be reached, the bond energy ϵ must be large enough, so that detachment of atoms from the islands is expected to be negligible during the simulations. We analyze the final state, where there are no mobile atoms left.

The transition rate W for an atom to diffuse from a site to the next one is calculated with the METROPOLIS algorithm. Defining the energy variation ΔE between the final and the initial state for a given move, we choose $W=\exp(-\Delta E/k_BT)$ when $\Delta E \geqslant 0$, and $W=1$ when $\Delta E < 0$.

V. SCALING

When the final state is reached, we calculate the island-size distribution function N_s (defined as the concentration of islands with size s). From mass conservation, we have

$$\sum_{s=1}^{\infty} sN_s = \theta. \tag{7}$$

The total density of islands N is given by $N=\Sigma_{s\geqslant 2}N_s$ and the average island size is

$$S = \frac{\sum_{s=1}^{\infty} sN_s}{\sum_{s=1}^{\infty} N_s} = \frac{\theta}{N+N_1}. \tag{8}$$

In the final state, when there is no monomer left, $N_1=0$ and $S_f=\theta/N_f$. From the hypothesis that there is only one characteristic length scale (the average island size S), the density of islands of size s is expected [5,24,25] to obey a scaling relation of the form $N_s \sim Cf(s/S)$, where f is a scaling function. Using Eq. (7) with this scaling form leads to [23]

$$N_s = \theta S^{-2} f(s/S). \tag{9}$$

Another quantity of interest is the island-island correlation function $G(r)$, which is the probability to have two islands separated by the distance r,

$$G(r) = \frac{2}{L}\sum_k \tilde{\sigma}_k \tilde{\sigma}_{k+r}. \tag{10}$$

Here k is the possible positions for the center of the island (k may be an integer or a half-integer), and $\tilde{\sigma}_k=1$ or 0 if the site k is, respectively, occupied or not occupied by an island. For large r, and in the absence of long-range order, $G(r) \rightarrow N^2$.

VI. RESULTS

We now present the results of the simulations. In the following, all energies and temperatures will be provided in eV and Kelvins, respectively. Figure 5 shows our results for the average island size S_f, at saturation (i.e., when there are no mobile atoms left) as a function of the elastic interaction parameter A. Models I and II exhibit similar results. Depending on the sign of A, two regimes are found: when $A<0$, the average island size S_f slightly increases for increasing $|A|$. When $A>0$, S_f decreases. The main difference between model I and model II is the quantitative variation of S_f in the repulsive regime. Indeed, larger variations are observed for model I.

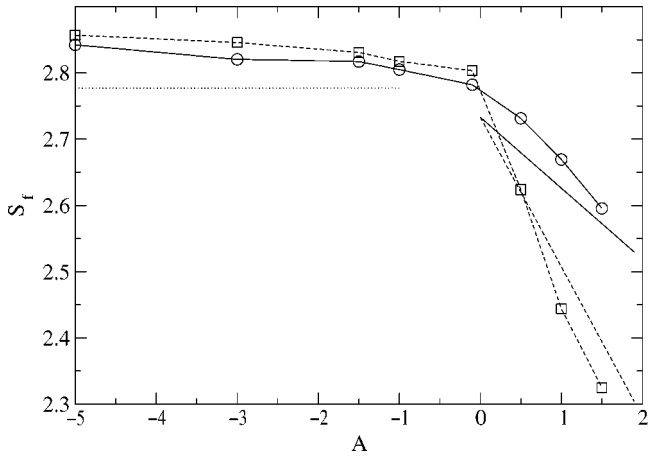

FIG. 5. Average island size S_f as a function of $A_{\|}$ for $L=1000$, $T=1000$, $\theta=0.1$, and $\epsilon=10$. Dashed lines for model I and solid lines for model II. Averages are taken over 500 realizations. The lines without symbols are the results of the mean-field model for model I and model II discussed in Sec. VII. The dotted line corresponds to the limit of strong attraction discussed in Sec. VII. The mean-field models reproduce the results of the simulations within 5% accuracy.

In Figs. 6 and 7, we provide the coverage dependence of the average island size. We have performed simulations on chains of $L=1000$ sites for $\theta \geqslant 0.1$ and $L=10\,000$ for $0.1 \geqslant \theta \geqslant 0.01$. These simulations were averaged over 500 runs. The interactions significantly change the average island size for intermediate coverages only. At high coverages $\theta \rightarrow 1$, S_f does not depend on the interactions. In the opposite limit at $\theta \rightarrow 0$, the island size seems to tend to a constant universal value $S_f \rightarrow 2.76 \pm 0.01$ which is also independent of the interactions.

The scaled island size distribution is plotted in Fig. 8, for coverage $0.01 < \theta < 0.6$, at saturation and for model I (model II leads to similar results). Using Eq. (9), we obtain a data collapse for both attractive and repulsive interactions when $\theta < 0.2$. Nevertheless, for large enough coverages, significant deviations from the scaling behavior are found. Indeed, the scaling function $f=N_sS_f^2/\theta$ exhibits more islands of large size in this regime. This breakdown of the scaling behavior indicates that there is more than one length scale which intervenes in the dynamics.

We have also computed the island correlation function $G(r)$, which is shown in Fig. 9. This function shows that no order appears in the distribution of islands, even when interactions are present. This result was checked for model I and model II for attraction and repulsion, as well as without interactions.

VII. MEAN-FIELD MODEL

A. Model equations

For the analysis of the above-mentioned results, we introduce a mean-field model which accounts for the interactions

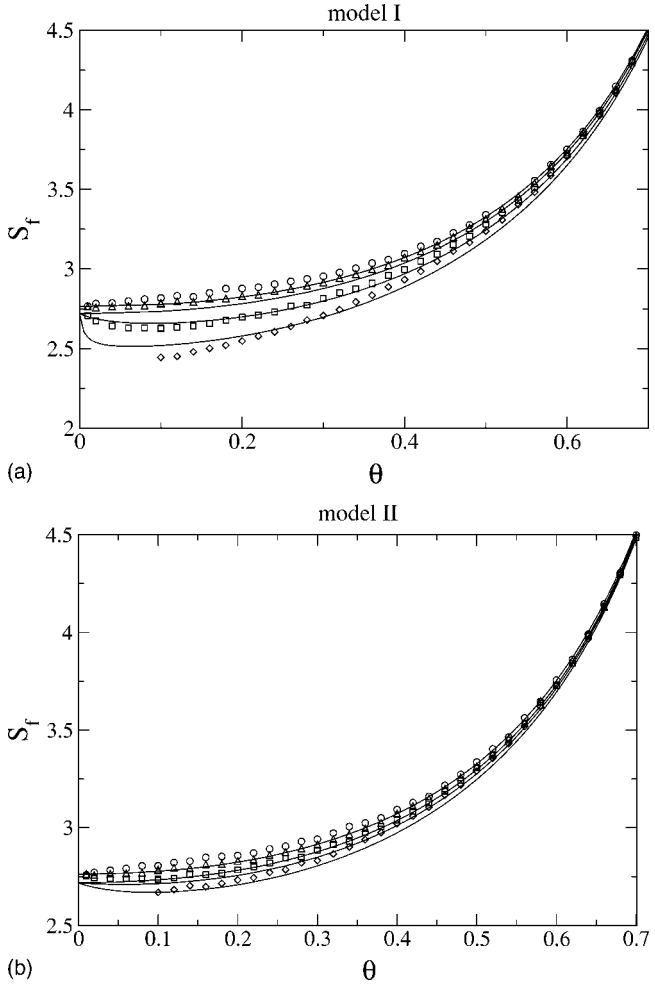

FIG. 6. Variation of the average island size with the coverage in the saturated lattice for $L=1000$, $T=1000$ K, and $\epsilon=10$ eV for model I and model II. Circles, triangles, squares, and diamonds correspond to $A=-1$, 0, 0.5, and 1 eV, respectively. The lines indicate the full solution of the mean-field model for the same values of A for $A>0$, and the limit of strong attraction of the mean-field model.

between the clusters via an adatom capture rate $k_{s,S}$ which depends both on the size of the cluster s and on the average island size S. Since the only mobile species are the monomers, and since islands cannot merge, the model reads

$$\partial_t N_s = N_1(k_{s-1,S}N_{s-1} - k_{s,S}N_s), \quad s > 1, \tag{11}$$

$$\partial_t N_1 = -N_1\sum_{s=1}^{\infty} k_{s,S}N_s - k_{1,S}N_1^2, \quad s = 1. \tag{12}$$

The challenge is now to evaluate $k_{s,S}$ from microscopic dynamics.

B. No interaction

When there is no interaction, we shall assume that the attachment rates are independent of the size s of the islands. Nevertheless, $k_{s,S}$ may depend on the average island size S,

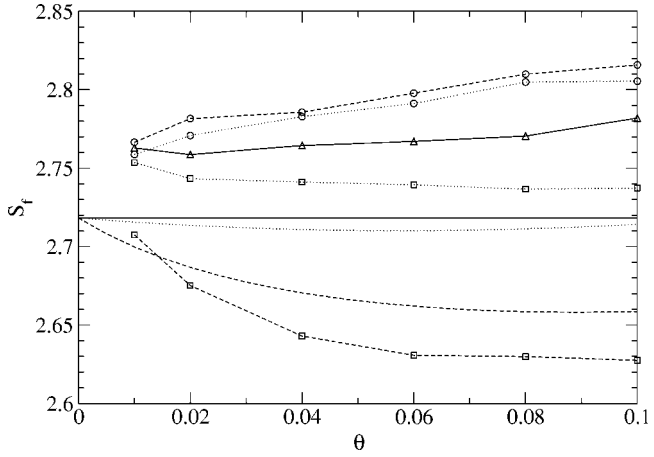

FIG. 7. Variation of the average island size for low coverages, with $T=1000$ K and $\epsilon=10$ eV for model I (dashed lines) and model II (dotted lines). Circles, triangles, and squares correspond to $A=-1$, 0, and 0.5 eV, respectively. The lines without symbols indicate the solution of the mean-field model without interactions and for $A=0.5$.

which contains information about the typical distance on which an atom diffuses before reaching an attachment site. Therefore, one may write $k_{s,S}=P_S$. Assuming random deposition of the atoms with probability θ at each site as an initial condition, the mean-field model Eqs. (11) and (12) is solved in Appendix B. This leads to a final average cluster size which does not depend on P_S. Indeed, P_S only determines how fast the global evolution occurs. We find

$$S_f^0 = \frac{e^{1-\theta}}{1-\theta}. \tag{13}$$

This result is in good agreement with the simulations, as shown in Fig. 6. For small θ, one has $S_f^0=e(1+\theta^2/2)$, in

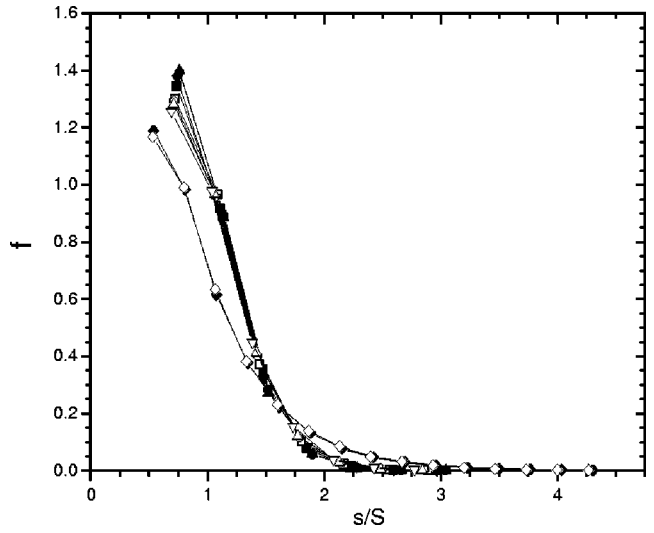

FIG. 8. Model I: Scaled size distributions in the saturated lattice for a coverage range of $0.01\leqslant\theta\leqslant0.2$ and $\theta=0.6$ for $L=10\,000$ and $T=1000$. The empty symbols correspond to $A_{\|}=-1$ and the filled ones to $A_{\|}=0.5$. For the sake of clarity, we have not plotted the case without interactions, which leads to similar results, with scaling functions between the attractive and repulsive case.

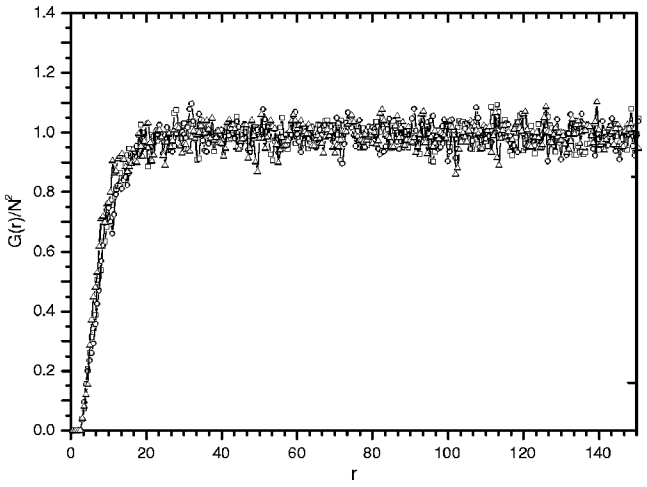

FIG. 9. Model I: Correlation function in the saturated lattice for a coverage range of $\theta=0.1$ and $A_{\|}=0.5$, 0, and -1, for $L=10\,000$ and $T=1000$.

agreement with Ref. [23], which indicate that $S_f \sim \theta^z$ with $z=0$ (i.e., S_f is constant) when $\theta \to 0$.

C. Repulsive interactions

We now consider the case where interactions are present. Due to the interaction with all clusters of the chain, the energy landscape experienced by a diffusing adatom is complex. Nevertheless, the interaction energy between atoms and clusters decreases with the distance as $1/r^3$, and as a first approach, we shall only account for the first neighbors of an adatom. In Appendixes A and B, the interaction energy of an adatom with a single cluster is calculated. As expected, we generically find a long-range attraction or repulsion when A is positive or negative.

We now assume that

$$k_{s,S} = 2P_S \pi_{s,S}, \tag{14}$$

where P_S is an attempt frequency which does not depend on s. $\pi_{s,S}$ is the probability for an atom between an island of size s and another island of size s_1 to attach to the cluster of size s, averaged over the size s_1. In this definition, the distribution of probability of s_1 is the time-dependent global distribution of islands in the system. We use an approximate expression for $\pi_{s,S}$ which is the probability for atoms to attach to a cluster of size s when the neighboring cluster has the average size S. In addition, we shall assume that the monomer starts exactly half-way between the two clusters. In the case without interaction, we then find that $\pi_{s,S}=1/2$, and one retrieves the expression of the previous section $k_{s,S}=P_S$.

The splitting probability for an atom between a cluster of size s at $L=0$ and a cluster of size S at $L=\ell$ is [26]

$$\pi_{s,S} = \frac{\int_{\ell/2}^{\ell} dL \exp[U(L)/k_BT]}{\int_0^{\ell} dL \exp[U(L)/k_BT]}, \tag{15}$$

where ℓ is the distance between the clusters and U is the potential experienced by the adatom between the two clusters. Instead of analyzing directly Eq. (15), we will use approximated expressions in the following, which will make the physical ingredients more explicit.

In the regime where clusters and atoms repel each other ($A_{\|}>0$ or $A_{\perp}>0$), an adatom has to cross an energy barrier E_s to attach to a cluster starting from a reference state far from the island where $U=0$. The energy barrier for attachment of an atom to an island is calculated in Appendixes A 1 and A 2. For model I, we have

$$E_s = A_{\|} \frac{s(s+3)}{2(s+1)(s+2)}. \tag{16}$$

As shown in Appendixes A 1 and A 2, islands-adatoms and adatoms-adatoms interactions are $\sim 1/r^3$. Since the integral of $1/r^3$ converges, one can consider that the interaction has a finite range, as opposed, for example, to $1/r$ interactions, which have an infinite range. It is therefore reasonable to assume that the interaction between an island and an atom is negligible at a distance larger than $\tilde{a}$ (which is on the order of several atomic distances). Since the integrands in Eq. (15) are proportional to $\exp(U/k_BT)$, they vary rapidly with the value of U. Taking the reference energy to be zero on the terrace far from the island, one has $\exp(U/k_BT) \approx 1$ in this region, and $\exp(U/k_BT) \approx \exp(E_S/k_BT)$ close to an island. A simple approximation for Eq. (15) is therefore

$$\pi_{s,S} \approx \frac{\tilde{a}\exp(E_S/k_BT) + \ell/2}{\tilde{a}\exp(E_S/k_BT) + \tilde{a}\exp(E_S/k_BT) + \ell} \approx \frac{\theta \exp(E_S/k_BT) + 1/2}{\theta[\exp(E_s/k_BT) + \exp(E_S/k_BT)] + 1}. \tag{17}$$

Since $\tilde{a}$ is of the order of atomic distances, we can write that $\tilde{a}/\ell \sim \theta$, which leads to the second expression in Eq. (17).

As a rough approximation, we linearize Eqs. (14), (16), and (17) for $(s-S)$ small, and obtain $\pi_{s,S}=(1/2)[1+Q_S(s-S)]$, with $Q_S = 2\partial_s \pi_{s,S}|_{s=S}$. Using Eq. (14), we finally get

$$k_{s,S} = P_S[1 + Q_S(s-S)], \tag{18}$$

where Q_S is a function of S. In the present case where interactions are repulsive, we find

$$Q_S = -\frac{\theta \partial_S E_S/k_BT}{2\theta + \exp(-E_S/k_BT)}. \tag{19}$$

The mean-field model (11) and (12) with arbitrary Q_S in Eq. (18) is solved analytically in Appendix B. Linearizing the solution for small Q_S, we find the final average island size,

$$S_f = S_f^0 \left(1 - \int_{(1-\theta)^{-1}}^{S_f^0} \frac{dS}{S} \int_{(1-\theta)^{-1}}^{S} dS'(S'^{-1} - 1) Q_{S'} \right), \tag{20}$$

where S_f^0, given in Eq. (13), is the average island size in absence of interactions. Once again, we find that P_S has no influence on S_f. As shown in Figs. 5 and 6, Eq. (20) reproduces the results of the simulations within better than 5% accuracy.

We might first notice that when $\theta \to 0$, one has $Q_S \to 0$, and it follows that $S_f \to e$ for any interaction constant. In-

deed, the distances between adatoms and islands diverge in the limit of low coverages. Therefore, the diffusion from one island to the other takes a much longer time than the attachment to an island or to another atom. In this limit, the kinetics is limited by diffusion, and the interactions have no consequences on the evolution of the system. From Eq. (17) one can easily find that the universal diffusion-limited regime is reached when $\theta < \theta^* = \exp(-E_S/k_BT)$. These results are in agreement with the simulations, where we have found that $S_f \to 2.76 \pm 0.01$ when $\theta \to 0$ for all values of the interaction. The crossover to the diffusion-limited regime in the simulations is seen for $\theta^* \approx 0.1$ when $A_\parallel = 0.5$ eV and $T = 1000$ K. Considering that the limiting process is that of dimer formation, we indeed find that $\theta^* \approx \exp(-E_1/k_BT) \approx 0.1$.

In the opposite limit $\theta > \theta^*$, the attachment dynamics is a standard Arrhenius law limited by the attachment barriers E_s,

$$\pi_{s,S} = \frac{\exp(-E_s/k_BT)}{\exp(-E_s/k_BT) + \exp(-E_S/k_BT)}, \tag{21}$$

which leads to $Q_S = -(1/2)\partial_S E_S/k_BT$. In the low coverage limit of this regime $\theta^* < \theta \ll 1$, the final average island size given by Eq. (20) does not depend on the coverage θ and takes a simple form,

$$S_f \approx e - 0.02(A_\parallel/k_BT). \tag{22}$$

In the limit $\theta \to 1$, the final configuration is mainly dictated by the initial conditions. Therefore, it is once again independent of the interactions, and we find that $S_f \to S_f^0 \approx 1/(1-\theta)$.

For model II in the repulsive regime ($A_\perp > 0$), and when ϵ is large (which corresponds to the limit of irreversible aggregation), the attachment energy barrier is

$$E_s = A_\perp \sum_{i=2}^{s+1} \frac{1}{i^3}. \tag{23}$$

Approximating E_s by a continuous integral ($E_s \approx A_\perp \int_{3/2}^{s+3/2} dx/x^3$), and following the same lines as for model I, the mean-field model is solved with energy barriers given by Eq. (23).

Once again, the result is given by Eq. (20), and the diffusion-limited regime $S_f \to e$ is recovered for $\theta < \theta^*$. We also retrieve the limit of high coverage $S_f \approx 1/(1-\theta)$ when $\theta \to 1$. At intermediate coverages $\theta^* < \theta \ll 1$, we find

$$S_f \approx e - 0.01(A_\perp/k_BT), \tag{24}$$

which, as compared to model I [Eq. (22)], indicates a weaker decrease of the average island size with the interaction strength. This result is confirmed by the simulations reported in Fig. 5. This seems *a priori* surprising since the long-range interaction takes exactly the same form in both models: As/r^3, where s is the island size, and $A = A_\parallel$ or $A_\perp$. This result in fact confirms that the dynamics is controlled by the model-dependent energy barriers E_s rather than by the asymptotic behavior of the interactions.

D. Attractive interactions

Let us now consider the case of attractive interactions ($A_\parallel < 0$ or $A_\perp < 0$). The potential experienced by an adatom exhibits a maximum somewhere between the two neighboring clusters, and decreases when approaching one of these clusters (see Fig. 11 and Appendixes A 1 and A 2).

When the attraction is strong enough, the potential experienced by a mobile atom is very steep, and the atom always moves towards the direction where the potential decreases. Therefore, the dynamics is deterministic, and the probability for an adatom to attach to a cluster of size s when the neighboring cluster has a size S is the probability for the adatom to be between the cluster of size s and the maximum of the potential seen by the adatom $U \sim A[sL^{-3} + S(\ell - L)^{-3}]$. This potential is the same for model I and model II. We have defined ℓ as the distance between the clusters, and L as the distance to the cluster of size s. Assuming that the initial position of the adatom is random, we find that $\pi_{s,S}$ is the ratio of the distance between the maximum of the potential and the island of size s, called $L_{\max}$, over the distance between the clusters ℓ. Since $L_{\max} = \ell/[1 + (S/s)^{1/4}]$ does not depend on the strength of the interactions A, the probability $\pi_{s,S}$ also does not depend on A. We find

$$\pi_{s,S} = \frac{L_{\max}}{\ell} = \frac{1}{1 + (S/s)^{1/4}}. \tag{25}$$

Expanding for $(s - S)$ small and assuming once again that $k_{s,S} = 2P_S\pi_{s,S}$, we find $Q_S = q/S$, where $q = 1/8$. Using Eq. (20), we obtain an expression for the final average island size in the limit of infinitely strong attraction,

$$S_f = \frac{e^{1-\theta}}{1-\theta} + q\left(\frac{1+\theta}{2}e^{1-\theta} - 1\right) + o(q^2) \tag{26}$$

with $q = 1/8$. The first term of Eq. (26) corresponds to the case without interactions. The second term is positive and small. Equation (26) therefore suggests a small increase of S_f when the attraction increases, up to a limit value. The prediction of the mean-field model Eq. (26) is plotted together with the simulation results ofFig. 6. Once again, good agreement is found with the simulations. As opposed to the case of repulsive interactions discussed in the previous section, the dynamics here is solely dictated by the asymptotic behavior of the potential at long distances, which is identical for model I and model II. This explains why these models lead to identical results in the presence of strong attractive interactions.

Moreover, as mentioned for the case of repulsive interactions, one should recover the universal diffusion-limited regime where S_f does not depend on the interactions for low enough coverages (or weak enough interactions), when $\theta \ll \exp(E_S/k_BT)$. This result is indeed observed in the simulations in Fig. 6.

VIII. DISCUSSION

We would now like to draw the attention of the reader to the limit of low coverages. Many authors in the literature

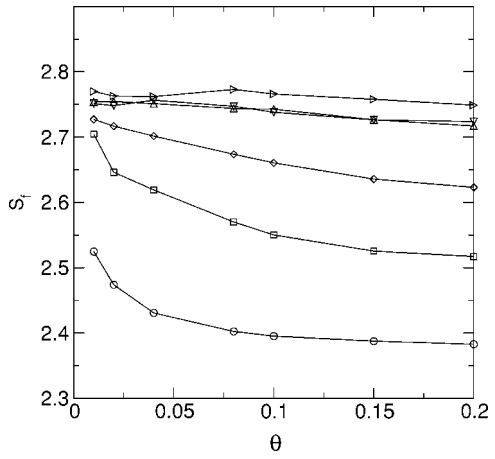

FIG. 10. Point island model, low coverage behavior of the final average island size. From top to bottom, the curves correspond to values of the repulsive interaction $A_p/k_BT=-1$, 0, 0.1, 1, 2, and 4.

[11,15,23] introduce an exponent z from the relation $S\sim\theta^{-z}$ when $\theta\to 0$. If z is nonvanishing, S_f should either diverge or vanish (depending on the sign of z) at low enough coverages. But it is clear that $S_f\geqslant 2$ because the smallest islands are dimers. Therefore, $z<0$ is impossible, and we must have $z\geqslant 0$. The mean-field model of the previous section predicts that S_f tends to a finite value in the limit of low coverages. This would indicate that $z=0$.

The limit $\theta\to 0$ is in fact very difficult to check, and we do not know of any study in the literature where S_f is obtained from simulations over several orders of magnitude for $\theta\to 0$. In order to check the robustness of our results, we have performed simulations at low coverages with a point island model. In this model, all atoms interact with each other with a dipolar interaction A_p/r^3. The interaction potential between an adatom and an island of size s is therefore sA_p/r^3. We also use the METROPOLIS algorithm, and attachment to a cluster is irreversible.

We have performed simulations at low coverage only (i.e., $\theta<0.2$), where the point island model is expected to be valid. The results, reported in Fig. 10, are once again consistent with the existence of a universal value of $S_f\to 2.75\pm 0.02$ at small coverages, which is the same as that obtained from the extended island model. Moreover, the saturation of the increase of S_f in the attractive regime is similar to that observed in the case of extended islands. For the repulsive regime, the behavior is similar to that of the extended island models, although quantitatively different.

In the absence of interaction, and in the presence of attractive interactions, the predictions of the mean-field model are in agreement with the simulations of the point island model. Nevertheless, they are quantitatively not accurate in the repulsive regime. This discrepancy may be due to the faster variation of the attachment barrier in the point island model $[E_s=s(A_p/k_BT)]$, which questions the validity of the linearization of $k_{s,S}$.

IX. CONCLUSIONS

We have analyzed irreversible aggregation in one dimension in the presence of elastic interactions between the particles. Two models were considered: a vectorial force-force model (model I) and a dipole-dipole model (model II). These models were analyzed both with Monte Carlo simulations and with the help of a mean-field model. Despite the very rough approximations used to design the mean-field model, its predictions reproduce the final average island size S_f obtained from the simulations within better than 5% accuracy. Let us now summarize the main results.

The distribution of islands exhibits a scaling behavior $N_sS^2/\theta=f(s/S)$ for low coverages, but not at high coverages. Moreover, the correlation functions of the spatial distribution of clusters reveal no order.

For both model I and model II, the limits of low and high coverage do not depend on the interactions. In the low coverage limit, the dynamics is diffusion-limited, and the average island size tends to a universal value $S_f=2.76\pm 0.01$. In the high coverage limit, the island distribution is essentially determined by the initial conditions, and $S_f\approx 1/(1-\theta)$ with random initial conditions.

For intermediate coverages, S_f depends on the interactions. We have obtained an asymmetric behavior as a function of the interaction strength. Indeed, the average island size decreases with repulsive interactions, but increases only slightly and saturates in the presence of attractive interactions. Significant quantitative differences between model I and model II are observed only for repulsive interactions.

A detailed analysis shows that dynamics is controlled by the long-distance asymptotic behavior of the interaction potential in the attractive regime, which is the same for all the models that we have studied (model I, model II, or the point island model). Therefore, S_f does not depend on the precise model for attractive interactions. On the contrary, S_f is determined essentially by the model-dependent attachment barrier at the border of the islands in the repulsive regime. This explains why we have obtained quantitative differences between different models in this regime.

To conclude, we shall mention that our study allows one to identify the relevant ingredients which control the nucleation dynamics. For example, we have found that the control of the average island size of the aggregates can be achieved only by tuning repulsive interactions at intermediate coverages (which is the only regime where significant variations of S_f have been observed).

APPENDIX A: ADATOM-CLUSTER INTERACTIONS

We analyze here the interactions between a cluster and an isolated atom (adatom). The qualitative behavior of the elastic contribution to the interaction energy is given in Fig. 11. A detailed analysis is given in the following.

1. Model I

In the case of force-force interactions, the total energy of a system with one adatom and one cluster containing s_C atoms is

$$E_{\text{tot}}(L,s)=E_C+E_A+E_{AC}, \tag{A1}$$

where E_C and E_A are, respectively, the self-energies of the cluster and the adatom, and E_{AC} is the interaction energy

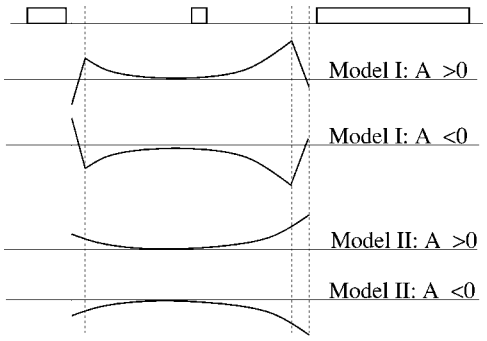

FIG. 11. Elastic contribution to the energy landscape experienced by a mobile atom between two clusters.

between the adatom and the cluster. L is the distance betweeen the center of the cluster and the center of the adatom. The self-energy of a cluster containing s atoms is

$$E^{\text{self}}(s) = -\epsilon(s-1) + \frac{A}{s}. \tag{A2}$$

One therefore has $E_C = E^{\text{self}}(s = s_C)$ and $E_A = E^{\text{self}}(s=1)$. The interaction energy between the cluster and the adatom is

$$E_{AC} = \frac{2A_{\parallel} L s_C}{[L^2 - (s_C-1)^2/4][L^2 - (s_C+1)^2/4]}. \tag{A3}$$

When the adatom is far from the island (i.e., $L \gg s_C$), one has $E_{AC} \sim A_{\parallel} s_C / L^3$. Finally, when the adatom attaches to the cluster, the total energy is simply $E_{\text{tot}} = E^{\text{self}}(s_C+1)$.

The total energy is plotted in Fig. 12 for various values of $A_{\parallel}$ and ϵ. We only consider the case $\epsilon > 0$. When $A_{\parallel} > 0$, there is a long-range repulsion between the adatom and the cluster. When $A_{\parallel} < 0$, there is a long-range attraction.

Nevertheless, there is a short-range repulsion of elastic origin when $A_{\parallel} < 0$ and ϵ is small. This effect is not relevant for our simulations which are performed in the irreversible limit, where $\epsilon > A_{\parallel}$.

2. Model II

We now consider dipole-dipole interactions. The total energy is once again given by Eq. (A1). Nevertheless, one has now

$$E_{AC} = A_{\perp} \sum_{i=1}^{s_C} \frac{1}{[L + (s_C+1)/2 - i]^3} \tag{A4}$$

and

$$E^{\text{self}}(s_C) = -\epsilon(s_C - 1) + A_{\perp} \sum_{i=1}^{s_C - 1} \frac{s_C - i}{i^3}. \tag{A5}$$

Contrary to the case of force-force interactions, we now have a monotonous contribution of the elastic interaction as a function of L. Therefore, $A_{\perp} > 0$ and $A_{\perp} < 0$ respectively lead to a repulsion and an attraction. These results are reported in Fig. 13.

APPENDIX B: MEAN-FIELD MODEL

We present a general solution of the mean-field model Eqs. (11) and (12) when

$$k_{s,S} = P_S[1 + Q_S(s - S)], \tag{B1}$$

where P_S and Q_S are functions of S [27]. Using Eq. (B1) in the mean-field model Eqs. (11) and (12), we extract two coupled evolution equations:

$$\partial_t N = P_S N_1^2 \left[1 + Q_S \left(1 - \frac{\theta}{N_1 + N} \right) \right], \tag{B2}$$

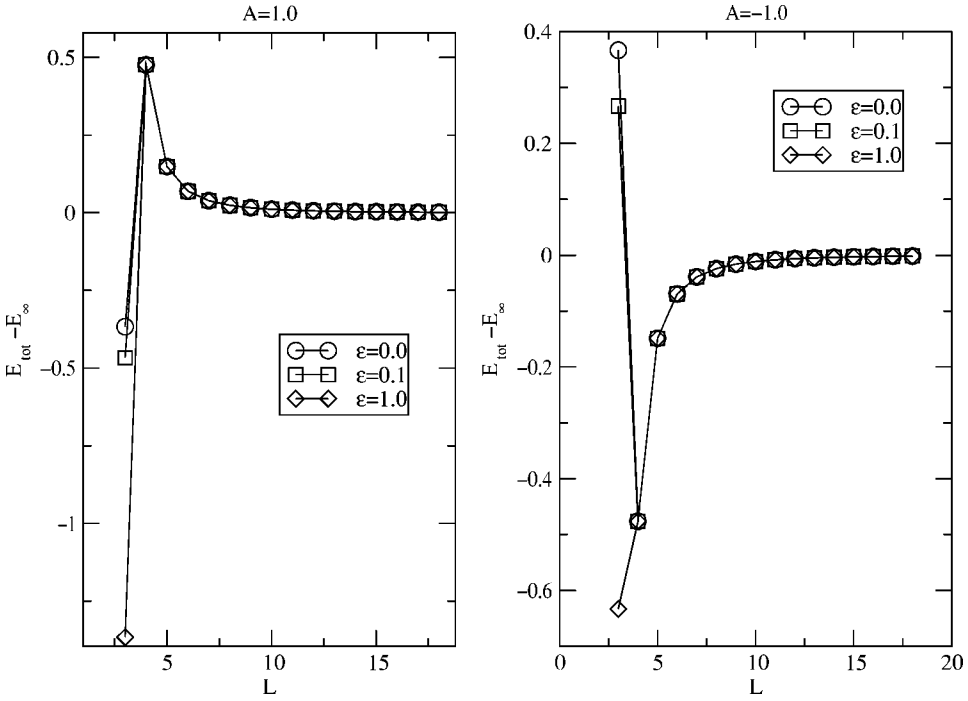

FIG. 12. Force-force model: Energy landscape $E_{\text{tot}} - E_{\infty}$ experienced by a diffusing adatom as a function of its distance L to the center of a cluster of five atoms.

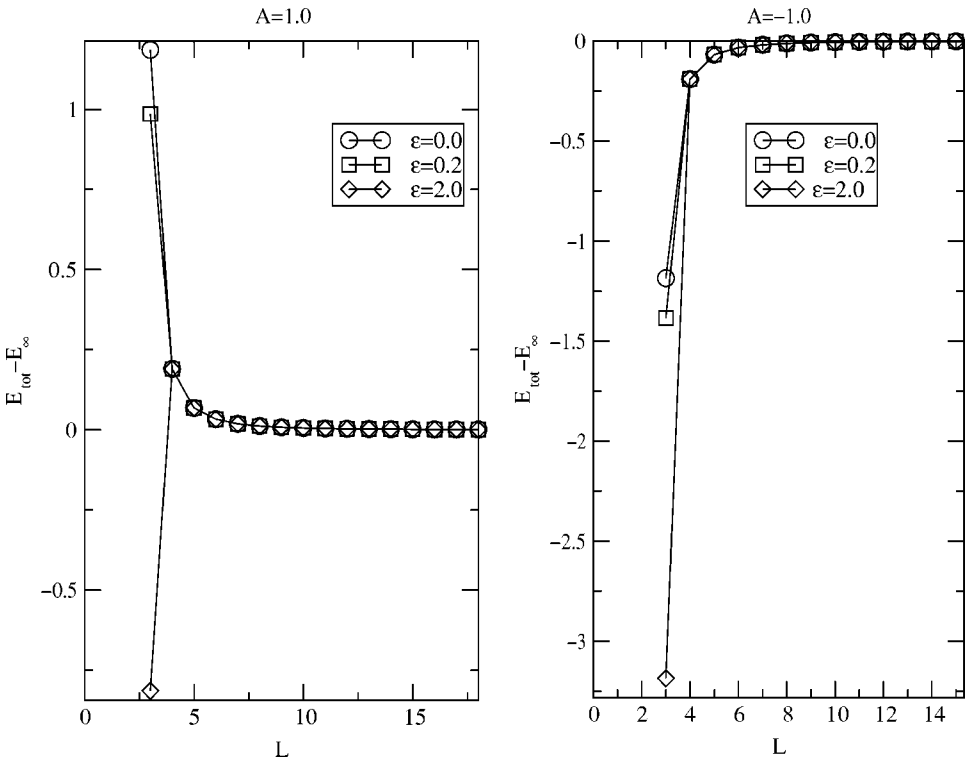

FIG. 13. Dipole-dipole model: Energy landscape $E_{\mathrm{tot}}-E_{\infty}$ experienced by a diffusing adatom as a function of its distance L to the center of a cluster of five atoms.

$$\partial_t N_1 = -P_S(2+Q_S)N_1^2 - P_S N N_1 + P_S Q_S \theta \frac{N_1^2}{N+N_1}. \quad \text{(B3)}$$

The first step is to use a new time variable τ such that $\partial_t \tau = P_S N_1$. One can easily check that $M=N+N_1=\theta/S$ decays exponentially in the new time variable τ, and using the initial condition $N_1=N_1^i$ and $N=N^i$ at $t=0$ (corresponding to $\tau=0$), we get $M=M^i\exp(-\tau)$, where $M^i=N_1^i+N^i$. Since $S=\theta/M$, we have

$$S = (\theta/M^i)\exp(\tau). \quad \text{(B4)}$$

Using this result in the evolution equation for N_1, we find a first-order differential equation with nonconstant coefficients, which can be put in the form

$$\partial_\tau[N_1 \exp(\tau+g)] = -M^i \exp(g), \quad \text{(B5)}$$

where

$$\partial_\tau g = Q_S[1-(\theta/M^i)\exp(\tau)]. \quad \text{(B6)}$$

Integrating this relation and using the condition for the final state $N_1=0$, $\tau=\tau_f$, we find

$$N_1^i \exp(\, g|_{\tau=0}) = M^i \int_0^{\tau_f} d\tau \exp(g), \quad \text{(B7)}$$

which is an implicit equation from which τ_f can be extracted. Finally, the final average island size is found from Eq. (B4): $S_f=(\theta/M^i)\exp(\tau_f)$.

A linearization of this model for Q_S small leads to

$$S_f = \frac{\theta}{M^i} e^{N_1^i/M^i}\left(1+\frac{N_1^i}{M^i}\, g|_{\tau=0} - \int_0^{N_1^i/M^i} d\tau g\right) + o(Q_S^2). \quad \text{(B8)}$$

Let us now determine the initial conditions which correspond to our simulations. We have deposited atoms on each site of the chain with a probability θ. The resulting coverage is $\theta=\Sigma_{s=1}^{\infty} s N_s$. The initial density of monomers is the probability to have a monomer at a given site times the probability not to have a monomer at the neighboring sites on both sides,

$$N_1^i = \theta(1-\theta)^2. \quad \text{(B9)}$$

The initial density of islands is the initial density of left ends of islands. Therefore, $N^i=\theta^2(1-\theta)$. We then deduce

$$M^i = \theta(1-\theta). \quad \text{(B10)}$$

Changing the integration variable from τ to S in Eq. (B8) and using the initial conditions mentioned above lead to Eq. (20).

[1] A. Pimpinelli and J. Villain, *Physics of Crystal Growth* (Cambridge University Press, Cambridge, 1998).
[2] J. A. Venables, G. D. Spiller, and M. Handbucken, Rep. Prog. Phys. **47**, 399 (1984).
[3] S. Stoyanov and D. Kashchiev, *Thin Film Nucleation and Growth Theories: A Confrontation with Experiment*, in Current Topics in Material Science, edited by E. Kaldis (North Holland, Amsterdam, 1981), Vol. 7, p. 69.
[4] G. S. Bales and D. C. Chrzan, Phys. Rev. B **50**, 6057 (1994).
[5] M. C. Bartelt and J. W. Evans, Phys. Rev. B **46**, 12 675 (1992).
[6] P. Gambardella, M. Blanc, H. Brune, K. Kuhnke, and K. Kern, Phys. Rev. B **61**, 2254 (2001).
[7] F. J. Himpsel *et al.*, Solid State Commun. **117**, 149 (2001).
[8] Z. Gai, G. A. Farnan, J. P. Pierce, and J. Shen, Appl. Phys. Lett. **81**, 742 (2002).
[9] Adam Li *et al.*, Phys. Rev. Lett. **85**, 5380 (2000).
[10] K. H. Lau and W. Kohn, Surf. Sci. **65**, 607 (1977).
[11] O. Tataru, F. Family, and J. G. Amar, Physica A **273**, 231 (1999).
[12] J. Steinbrecher, H. Muller-Krumbhaar, E. Brener, C. Misbah, and P. Peyla, Phys. Rev. E **59**, 5600 (1999).
[13] G. Indiveri, E. Scalas, A. C. Levi, and A. Gliozzi, Physica A **273**, 217 (1999).
[14] F. Gutheim, H. Muller-Krumbhaar, and E. Brener, Phys. Rev. E **63**, 041603 (2001).
[15] B. M. T. Gonçalves and J. F. F. Mendes, Phys. Rev. E **65**, 061602 (2002).
[16] B. Houchmandzadeh and C. Misbah, J. Phys. I **5**, 685 (1995).
[17] P. Peyla and C. Misbah, Eur. Phys. J. B **33**, 233 (2003).
[18] M. Giesen, Prog. Surf. Sci. **68**, 1 (2001).
[19] G. Jin, J. L. Liu, S. G. Thomas, Y. H. Luo, K. L. Wang, and B.-Y. Nguyen, Appl. Phys. A: Mater. Sci. Process. **70**, 551 (2000).
[20] Q. Gong, R. Notzel, H.-P. Schönherr, and K. H. Ploog, Physica E (Amsterdam) **13**, 1176 (2002).
[21] G. Rosenfeld, R. Servaty, C. Teichert, B. Poelsema, and G. Comsa, Phys. Rev. Lett. **71**, 895 (1993).
[22] B. Muller, L. Nedelmann, B. Fischer, H. Brune, and K. Kern, Phys. Rev. B **54**, 17 858 (1996).
[23] Ji Li, A. G. Rojo, and L. M. Sander, Phys. Rev. Lett. **78**, 1747 (1997).
[24] F. Family and P. Meakin, Phys. Rev. Lett. **61**, 428 (1988).
[25] J. G. Amar, F. Family, and Pui-Man Lam, Phys. Rev. B **50**, 8781 (1994).
[26] N. G. Van Kampen, *Stochastic Processes in Physics and Chemistry* (North Holland, Amsterdam, 1992).
[27] Any linear function of s can be written in the form (B1).